Acousto-optic Modulation of Terahertz Radiation in Liquefied Sulfur Hexafluoride at Room Temperature

Pavel A. Nikitin[1,2] · Vasily V. Gerasimov[3,4] · Vitaly B. Voloshinov[2]

Abstract

Acousto-optic modulation of terahertz free-electron laser radiation was investigated using diffraction on an acoustic wave in liquefied sulfur hexafluoride at room temperature. At the wavelength 130 μm, the diffraction efficiency in Bragg regime of interaction 1% was obtained at 75 V driving electrical signal applied to the transducer terminals.

Keywords Acousto-optics · Terahertz radiation · Diffraction · Sulfur hexafluoride

1 Introduction

Nowadays there is an increasing interest in the electromagnetic radiation of the terahertz (THz) range, which is broadly used in science and technology [1]. One of the actual problems of the THz science is development of efficient and quick-action devices for controlling these radiation parameters. To modulate the intensity of THz radiation, a number of methods are used [2–5]. One of them is modulation due to changes in the conductivity of the material when it is illuminated by visible laser radiation. This method allows one to control THz radiation in the range from 0.25 to 1 THz and is characterized by the modulation speed from 0.1 kHz to 1 MHz and requires pump power of the laser radiation from 10 mW to several watts. Another method is to change the conductivity of semiconductor heterostructures or metamaterials when the electric voltage is applied. The main drawback of this method

✉ Pavel A. Nikitin
nikitin.pavel.a@gmail.com

1   Scientific and Technological Center of Unique Instrumentation RAS, Moscow, 117342, Russia

2   Faculty of Physics, Lomonosov Moscow State University, Moscow, 119991, Russia

3   Budker Institute of Nuclear Physics of SB RAS, Novosibirsk, 630090, Russia

4   Novosibirsk State University, Novosibirsk, 630090, Russia

is that the modulation speed is in the order of 1 kHz. Nevertheless, use of electrical modulation of THz radiation is simpler than optical modulation. One more method is mechanical tuning of a flexible substrate. Such modulators have better signal transmission or reflection than listed above. Unfortunately, they have low stability in the deformed state. Besides, modulation of THz radiation can be realized by employing the magneto-optical effect under an external magnetic field, leading to the extremely high modulation speed of about 1 GHz. However, such modulators are poorly controllable. In addition, intensive THz radiation may be modulated by microelectromechanical systems (MEMS), but they could be used exclusively at frequencies close to the resonance one and the modulation speed is limited to several kHz.

Among various optoelectronic methods of control, the acousto-optic (AO) methods of modulation of THz radiation seem really attractive as they enable:

– To control powerful radiation [6];
– Simultaneous modulation and deflection of radiation [6, 7];
– To control polarization of radiation;
– The modulation speed up to 1 MHz [7];
– The modulation depth up to 100% [8];
– High spectral resolution from 10 to 10^3 [7, 9];
– The possibility of tuning to a given radiation wavelength λ by changing the ultrasound frequency F ($\Delta\lambda/\lambda = \Delta F/F < 50\%$) [10].

Sounding advantages of the AO devices include compactness, high operating speed, absence of moving parts, and ability to control the transfer function by changing characteristics of the ultrasonic wave. AO devices have already proved their advantages in the ultraviolet, visible, and infrared ranges. However, there are only a few publications [8, 11, 12] devoted to AO control of THz radiation. This is due to the fact that the efficiency of Bragg diffraction I_1/I_0, equal to the ratio of the intensity I_1 of the radiation diffracted by ultrasound and the intensity I_0 of the radiation transmitted through the AO cell, is inversely proportional to the square of the radiation wavelength λ [11]:

$$\frac{I_1}{I_0} = \frac{\pi^2}{2\lambda^2}\frac{M_2 P_a}{d}L, \tag{1}$$

where d and L are the width and the length of the acoustic piezo-transducer; $P_a \propto U^2$ is the power of the acoustic wave, proportional to the square of the driving electrical signal voltage U; M_2 is the AO figure of merit. According to relation (1), the efficiency of the THz radiation diffraction at the typical values $M_2 = 100 \cdot 10^{-15}$ s^3/kg, $P_a = 1$ W, $d = 5$ mm, $\lambda = 100$ μm, and $L = 5$ cm is expected to be only $I_1/I_0 = 0.05\%$. Therefore, it was assumed that the AO effect would not find application in the THz range and, as a result, this field of investigations was practically ignored by specialists.

In [11], the AO diffraction of THz radiation ($\lambda = 119$ μm) on a longitudinal acoustic wave propagating along the crystallographic axis [100] of a germanium single crystal was studied. The observed diffraction efficiency reached 1.5%. This high

value of the diffraction efficiency was achieved due to the use of a standing acoustic wave, i.e., at fixed acoustic frequencies.

In [12], the investigation of AO diffraction of radiation at $\lambda = 119$ μm by ultrasound having $P_a = 150$ W was carried out. When using TPX (polymethylpentene) plastic, polyethylene, and germanium single crystal, the ratio $I_1/I_0^{(*)}$ was 0.07% (here, $I_0^{(*)}$ is the intensity of radiation incident on the AO cell). The AO interaction was not registered in crystal quartz because of its low value of the AO figure of merit M_2 in the THz range. In addition, AO diffraction was implemented in non-polar liquids: in carbon tetrachloride (CCl_4) and cyclohexane (C_6H_{12}), the ratio $I_1/I_0^{(*)}$ was about 0.5%.

To continue the research in this field, our team carried out a series of experiments [6, 7, 13] using a germanium single crystal and non-polar liquids as a medium of the AO interaction. Diffraction of THz radiation at $\lambda = 130$ μm was observed under the normal conditions, i.e., at room temperature and 1 bar atmospheric pressure. It was found that the value of M_2 of the liquids was a few times higher than that of the germanium single crystal. However, the maximum efficiency of the diffraction in the THz range on a travelling acoustic wave, obtained to date in the experiments using non-polar liquids and single crystals, was only $I_1/I_0 = 0.02\%$ per 1 W of acoustic power [6].

Therefore, to achieve a significant diffraction efficiency, it is necessary (1) to use a high-power acoustic wave and (2) to look for media transparent in the THz range with high AO figure of merit. The first way is physically limited due to the overheating and destruction of an AO cell material. Therefore, we explored the second possibility.

It is known that the AO figure of merit of liquids can be calculated by the following formula [6]:

$$M_2 = \left[\frac{(n^2 - 1)(n^2 + 2)}{6n} \right]^2 \frac{4}{\rho V^3}, \qquad (2)$$

where n is the refractive index, ρ is the density, and V is the sound velocity. From Eq. 2 one can see that the coefficient M_2 is inversely proportional to the cube of the sound velocity V. It was experimentally proved in [8] that the sound velocity in liquefied inert gases could be an order of magnitude lower than that in non-polar liquids under normal conditions. Therefore, as follows from Eq. 2, the AO figure of merit M_2 of a liquefied gas may be three orders of magnitude higher than that of non-polar liquid like cyclohexane.

Reference [8] is the only work in which the AO interaction in liquefied gases was realized. It was found that a liquefied sulfur hexafluoride (SF_6) was characterized by a significantly higher value of $M_2 = 15000 \cdot 10^{-15}$ s^3/kg as compared with that of liquefied noble gases (Ar, Kr, Xe). The AO figure of merit of SF_6 was expected to double with increase in the temperature from $t = 14°C$ to $t = 24°C$. However, the experiment in [8] showed that an increase in the temperature by 1°C, from $t = 13°C$ to $t = 14°C$, led to a significant decrease (3 times) of the diffraction efficiency. Therefore, in order to solve the mentioned contradiction, we have implemented AO diffraction of THz radiation in the liquefied sulfur hexafluoride at $t = 24°C$, that is close to room temperature. Taking into account the high selectivity of AO interaction with respect to the radiation wavelength, the experimental study was carried out using

a quasi-monochromatic radiation generated by the Novosibirsk free-electron laser (FEL) [14].

2 Experimental Setup

The block scheme of the experimental setup is shown in Fig. 1 and the cross section of the AO cell is shown in Fig. 2. All dimensions are in millimeters.

The intensity and polarization of the radiation of FEL 1 was controlled by the wire polarizer 2 and the set of calibrated silicon-based attenuators 3. The radiation wavelength was equal to $\lambda = 130$ μm, corresponding to the minimum absorption of the atmosphere in the transparent window 128–132 μm [15]. The THz beam diameter $D = 5$ mm was controlled by the iris diaphragm 4. The cuvette 5 for the implementation of the AO interaction was a round steel tube with the diameter 15 cm, the length 10 cm, and the wall thickness 3 mm. The TPX 6-mm-thick plastic windows were placed inside the cuvette on both flanges. The flanges had the thickness 3 cm, while the openings in the flanges were 100×10 mm^2. The beams of diffracted and transmitted radiation were focused by the kinoform lens 6 with diameter 8 cm and the focal length 8 cm. The lens was located at the distance 3 cm from the cuvette orthogonal to the zero-order diffraction beam. The radiation was recorded by the uncooled microbolometer array 7 of 320×240 pixels with a pixel size of 51 μm [16]. To prevent interference effects in the microbolometer array, the array was located at the distance 2 cm beyond the focal plane of the lens, i.e., at the distance 10 cm from the kinoform lens.

It follows from formula (1) that the diffraction efficiency is proportional to the length L of the transducer. Therefore, the acoustic transducer was made of monolithic polycrystalline lead zirconate titanate (PZT) piezoelectric ceramics having the dimensions $80 \times 8 \times 6$ mm^3 ($L = 80$ mm). The electrodes were set on the opposite faces 80×8 mm^2. The acoustic transducer was placed inside the cuvette, along the axis of the cylinder, right near the input optical window. Due to this, the AO interaction took place in the horizontal plane. A high-frequency electrical signal from the generator 8 (Rigol DG1022), the amplitude of which was increased by the amplifier 9 (AKTAKOM AVA-1745), was applied to the transducer. Data from
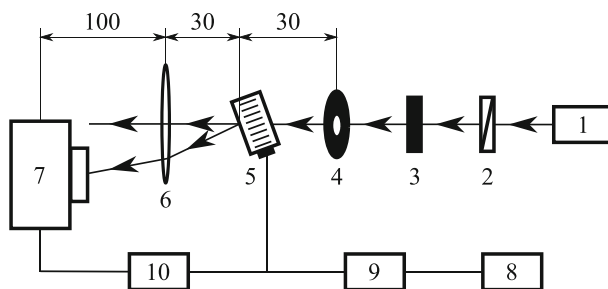

Fig. 1 Schematic of the experimental setup: (1) FEL; (2) polarizer; (3) set of calibrated attenuators; (4) aperture; (5) AO cell; (6) lens; (7) microbolometer array; (8) arbitrary waveform signal generator; (9) amplifier; (10) personal computer
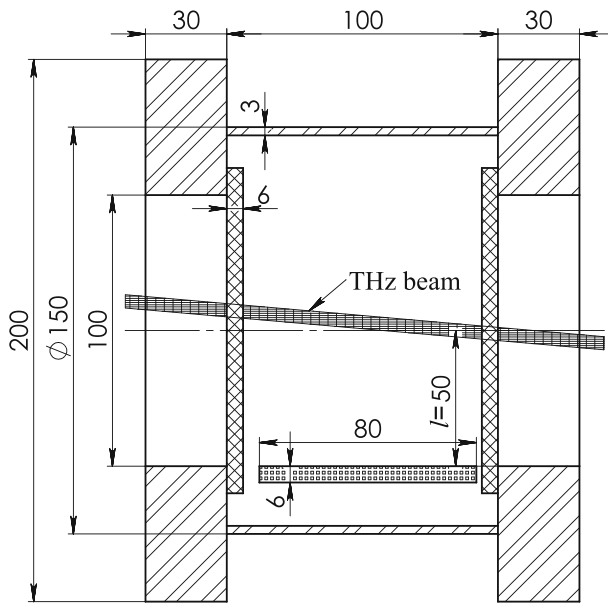
Fig. 2 Cross-section AO cell for liquefied sulfur hexafluoride

the microbolometer array 7 and the amplifier 9 were processed by the personal computer 10.

3 Results and Discussion

To demonstrate the AO modulation of the THz radiation, the dependence of the diffraction efficiency on time was measured (see Fig. 3). The measurements were carried out at the temperature $t = 24°C$ and the pressure $p = 24$ bar, the electrical signal applied to the piezoelectric transducer at the amplitude $U = 75$ V and the frequency $F = 328$ kHz having an envelope in the form of a meander with a frequency of 1 Hz.

The operating speed of the microbolometer array 7 was 40 μs (25 frames per second), and the propagation time of the sound wave across the THz beam $\tau = D/V \approx 25$ μs. Therefore, it was impossible to determine the rise time of the diffraction efficiency. It can be seen in Fig. 3 that during the duty cycle of the electric signal, the value of the diffraction efficiency I_1/I_0 fluctuated in the range $(0.65 - 0.75)\%$. In our opinion, these variations were related to the temporal intensity instability of the FEL THz radiation.

The obtained spatial distributions of the intensities of the transmitted (I_0) and diffracted (I_1) THz radiation beams are shown in Fig. 4. Since the diameters of these beams turned out to be a few times smaller than the size of the microbolometer array 7, the dependences in Fig. 4 were cropped to equal-size areas of 80 × 90 pixels and normalized with respect to the maximum value max(I_0). Note that in Fig. 4 the ordinate axis corresponds to the AO interaction plane.
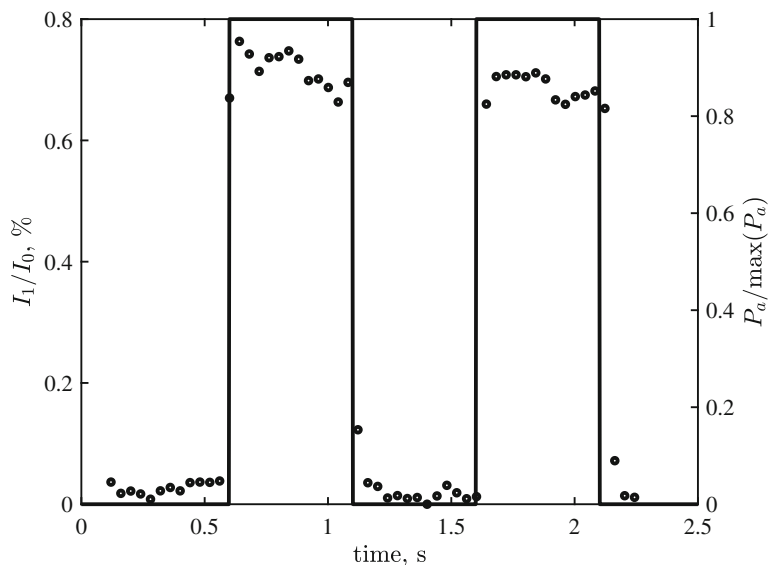
Fig. 3 Temporal dependencies of normalized acoustic power $P_a/\max(P_a)$ (line) and diffraction efficiency I_1/I_0 (dots)

From Fig. 4 one can see that the transmitted and diffracted THz radiation beams were extended perpendicular to the AO interaction plane. This is related to the undesirable side-effect of the radiation diffraction on the input and output openings in the flanges. The intensity in the central region of the diffracted beam was approximately 0.4% of $\max(I_0)$. To estimate the diffraction efficiency, the ratio of the integral intensities of the indicated beams was used. The calculation showed that about 0.7% of the transmitted radiation was deflected into the first diffraction order.
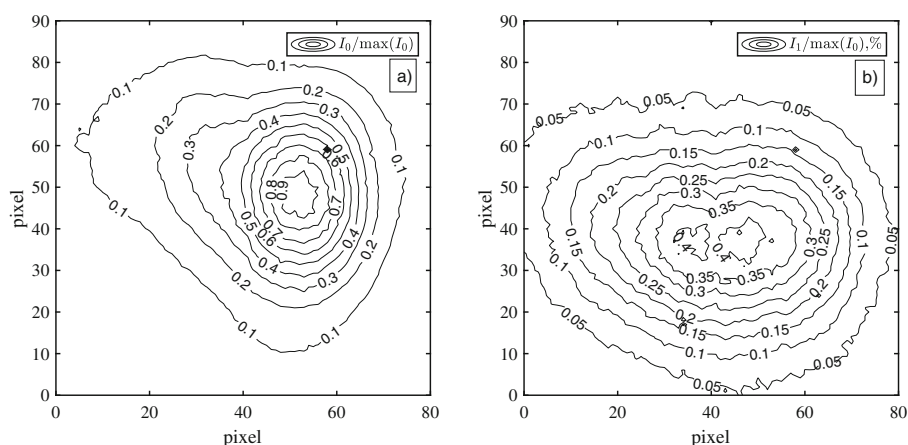

Fig. 4 Distribution of normalized radiation intensity in beam cross section. **a** Transmitted beam. **b** Diffracted beam

To compare the results obtained with the data in paper [8], it is necessary to take into account the attenuation of the acoustic wave $P_a \propto \exp(-\alpha_s l)$, as well as the temperature dependencies $M_2(t)$ and $\alpha_s(t)$ given in [8]. Here l is the distance at which the incident THz beam travels from the piezoelectric transducer. Therefore, the diffraction efficiency can be calculated in the following way:

$$I_1/I_0 = \text{const} \cdot \frac{M_2 U^2}{\lambda^2} \frac{L}{d} \exp(-\alpha_s l). \tag{3}$$

Below are the conditions of the experiments under which the weak AO interaction was observed:

–   In paper [4]: $t = 14°C$, $p = 28$ bar, $\lambda = 119\ \mu m$, $M_2 = 0.85 \cdot 10^4 \cdot M_2^{SiO_2}$, $\alpha_s = 0.32\ cm^{-1}$, $l = 2$ cm, $L = 180$ mm, $d = 10$ mm, $U = 150$ V, $I_1/I_0 = 2.7\%$;
–   In our work: $t = 24°C$, $p = 24$ bar, $\lambda = 130\ \mu m$, $M_2 = 2.05 \cdot 10^4 \cdot M_2^{SiO_2}$, $\alpha_s = 0.44\ cm^{-1}$, $l = 5$ cm, $L = 80$ mm, $d = 8$ mm, $U = 75$ V,

where $M_2^{SiO_2} = 1.51 \cdot 10^{-15}\ s^3/kg$ is the AO figure of merit of fused quartz.

It was found that under the conditions of our experiment, the diffraction efficiency should be about $I_1/I_0 \approx 0.16\%$. Note that this value is four times lower than the registered one. We suppose that this discrepancy is related to the fact that the AO figure of merit M_2 of liquefied sulfur hexafluoride at $t = 24°C$ is higher than predicted in [8]. Moreover, as we used a monolithic piezoelectric transducer, whereas in [8] a composite transducer was employed, the structure (amplitude and phase) of the sound beams might be different. This could affect the efficiency as well [17].

4 Conclusion

As a result of the study, we can conclude that under weak AO interaction in liquefied sulfur hexafluoride, an increase in temperature from 14 to 24°C leads to the higher diffraction efficiency of THz radiation. From which it follows that AO interaction in this liquefied gas can be simpler realized at room temperature rather than at lower temperatures requiring cooling.

References

1. I. Catapano and F. Soldovieri, *Chapter 11. THz Imaging and Data Processing: State of the Art and Perspective. In: Innovation in near-surface geophysics. (Elsevier), pp. 399–417*, 2019. https://doi.org/10.1016/b978-0-12-812429-1.00011-8.

2. M. Rahm, J.S. Li, and W. Padilla, *THz Wave Modulators: A Brief Review on Different Modulation Techniques*, Journal of infrared, millimeter, and terahertz waves **34** (2012), no. 1, 1–27. https://doi.org/10.1007/s10762-012-9946-2.

3. R. Degl'Innocenti, S. Kindness, H. Beere, and D. Ritchie, *All-Integrated Terahertz Modulators*, Nanophotonics **7** (2018), no. 1, 127. https://doi.org/10.1515/nanoph-2017-0040.

4. L. Wang, Y. Zhang, X. Guo, T. Chen, H. Liang, X. Hao, X. Hou, W. Kou, Y. Zhao, T. Zhou, S. Liang, and Z. Yang, *A Review of THz Modulators with Dynamic Tunable Metasurfaces*, Nanomaterials **9** (2019), no. 7, 965. https://doi.org/10.3390/nano9070965.

5. Z. Ma, Z. Geng, Z. Fan, J. Liu, and H. Chen, *Modulators for Terahertz Communication: The Current State of the Art*, Research **2019** (2019), 1. https://doi.org/10.34133/2019/6482975.

6. P. Nikitin, V. Voloshinov, V. Gerasimov, and B. Knyazev, *Acousto-Optic Modulation and Deflection of Terahertz Electromagnetic Radiation in Nonpolar Liquids*, Technical Physics Letters **43** (2017), no. 7, 635. https://doi.org/10.1134/s1063785017070112.

7. V. Voloshinov, P. Nikitin, V. Gerasimov, B. Knyazev, and Y. Choporova, *Deflection of a Monochromatic THz Beam by Acousto-Optic Methods*, Quantum Electronics **43** (2013), no. 12, 1139. https://doi.org/10.1070/qe2013v043n12abeh015195.

8. W. Durr, *Acousto-Optic Interaction in Gases and Liquid Bases in the Far Infrared*, International Journal of Infrared and Millimeter Waves **7** (1986), no. 10, 1537. https://doi.org/10.1007/bf01010756.

9. P. Nikitin. *A Review of Non-Polar Liquids as Materials for Bulk Acousto-Optic Devices Operating with Terahertz Radiation*. Journal of Physics: Conference Series. [accepted for publication in 2020].

10. S. Antonov, *Acousto-Optic Deflector Based on a Paratellurite Crystal Using Broadband Acoustic Adhesive Contact*, Acoustical Physics **63** (2017), no. 4, 410–415. https://doi.org/10.1134/s1063771017030010.

11. W. Durr and W. Schmidt, *Measurement of Acousto-Optic Interaction in Germanium in the Far Infrared*, International Journal of Infrared and Millimeter Waves **6** (1985), no. 10, 1043. https://doi.org/10.1007/bf01010680.

12. T. Vogel and G. Dodel, *Acousto-Optic Modulation in the Far-Infrared*, Infrared Physics **25** (1985), no. 1-2, 315. https://doi.org/10.1016/0020-0891(85)90097-1.

13. P. Nikitin, V. Voloshinov, V. Gerasimov, and B. Knyazev, *Deflection of Terahertz Vortex Beam in Nonpolar Liquids by Means of Acousto-optics*, Physics Procedia **84** (2016), 146. https://doi.org/10.1016/j.phpro.2016.11.026.

14. G. Kulipanov, E. Bagryanskaya, E. Chesnokov, Y. Choporova, V. Gerasimov, Y. Getmanov, S. Kiselev, B. Knyazev, V. Kubarev, S. Peltek, V. Popik, T. Salikova, M. Scheglov, S. Seredniakov, O. Shevchenko, A. Skrinsky, S. Veber, and N. Vinokurov, *Novosibirsk Free Electron Laser–Facility Description and Recent Experiments*, IEEE Transactions on Terahertz Science and Technology **5** (2015), no. 5, 798. https://doi.org/10.1109/tthz.2015.2453121.

15. S.B. Guo, K. Zhong, M.R. Wang, C. Liu, Y. Xiao, W.P. Wang, D.G. Xu, and J.Q. Yao, *Theoretical and Experimental study on Broadband Terahertz Atmospheric Transmission Characteristics*, Chinese Physics B **26** (2017), no. 1, 019501. https://doi.org/10.1088/1674-1056/26/1/019501.

16. Y. Choporova, B. Knyazev, and M. Mitkov, *Classical Holography in the Terahertz Range: Recording and Reconstruction Techniques*, IEEE Transactions on Terahertz Science and Technology **5** (2015), no. 5, 836. https://doi.org/10.1109/tthz.2015.2460465.

17. A. Trushin, P. Nikitin, and A. Muromets, *Acousto-Optic Interaction in TeO$_2$ and LiNbO$_3$ Devices with Surface Generation of Bulk Acoustic Waves*, AIP Conference Proceedings **1433** (2012), no. 1, 102. https://doi.org/10.1063/1.3703148.